Improved Uniformity in Tomographic Myocardial Perfusion Imaging with Attenuation Correction and Enhanced Acquisition and Processing

Luis I. Araujo, Jose M. Jimenez-Hoyuela, Joseph R. McClellan, Eugene Lin, Joseph Viggiano, and Abass Alavi

Division of Cardiology and Nuclear Medicine, University of Pennsylvania Health System, Philadelphia, Pennsylvania

Tissue attenuation results in nonuniform myocardial perfusion images with significant sex differences. New SPECT imaging protocols to correct attenuation are currently under investigation. This study was performed to assess the effects of attenuation correction (AC) on overall image uniformity compared with more conventional imaging protocols in both men and women. **Methods:** Thirty-nine patients (19 men, 20 women) with less than a 5% likelihood of coronary artery disease were studied. ^{99m}Tc-sestamibi studies were acquired with a triple-head scanner equipped with a simultaneous transmission and emission protocol. Four imaging protocols were compared: a 180° acquisition and filtered backprojection reconstruction (FBP), a 360° acquisition and FBP, a 360° acquisition and iterative reconstruction (IT), and a 360° acquisition with IT and AC. Quantitative analysis was performed to evaluate myocardial tracer uniformity for men and women. **Results:** 180°, 360° FBP, and 360° IT showed sex differences, with decreased tracer concentration in the anterior wall in women and decreased tracer concentration in the inferior wall in men. AC images showed the greatest uniformity (9.9% coefficient of variation for AC versus 12.5% for IT, $P < 0.0001$), and no statistically significant differences in uniformity were seen between male and female AC studies. **Conclusion:** More uniform myocardial perfusion images were obtained with AC, resulting in images with no differences in uniformity between men and women. These techniques are expected to improve specificity and overall diagnostic accuracy.

Key Words: SPECT; myocardial perfusion imaging; attenuation correction

J Nucl Med 2000; 41:1139–1144

Recent advances in myocardial perfusion imaging have improved the diagnostic sensitivity of this technique in the assessment of patients with known or suspected coronary artery disease. The use of SPECT results in an improved ability to localize defects (*1*). However, the specificity of perfusion imaging is suboptimal because of the effects of tissue attenuation on photons as they traverse the thoracic structures before detection by the gamma camera. Tissue attenuation results in nonuniform myocardial perfusion images with significant sex differences related to body habitus and leads to reduced accuracy of both tracer quantification and clinical interpretation (*2,3*). The physical properties of ^{99m}Tc-labeled radiopharmaceuticals, including higher energy levels and greater photon flux than with ^{201}Tl labeling, are better suited for imaging with current gamma cameras and have reduced the effects of tissue attenuation.

Attenuation correction (AC) in PET cardiac imaging has resulted in improved myocardial tracer distribution. Preliminary reports show PET myocardial perfusion imaging to have greater accuracy for diagnosis of coronary artery disease, mostly because of increased specificity (*4–6*). However, PET centers are not widely available, and PET myocardial perfusion imaging is still expensive. New developments in SPECT technology include acquisition protocols with 360° orbits and imaging processing as well as simultaneous acquisition of transmission and emission scans and AC myocardial perfusion images (*7–11*). The overall diagnostic accuracy of myocardial perfusion imaging may be improved with these enhanced modalities, especially AC (*12*). However, further evaluation of this technology is needed before its acceptance in routine clinical practice will become widespread.

This study was performed to assess the effects of new acquisition and processing techniques and AC on overall image uniformity compared with more conventional imaging protocols in both men and women.

MATERIALS AND METHODS

Patient Population

Thirty-nine patients (19 men, 20 women; age range, 22–54 y; mean age, 44.8 y) were included in this study. Average weight ranged from 77 to 118 kg (170–260 lb) for men and from 68 to 105 kg (150–230 lb) for women. None of the patients had a history of angina, hypertension, or diabetes. All patients had normal findings on physical examination and resting electrocardiography.

The reasons for testing included nonanginal chest discomfort in 27 patients, palpitations in 5, coronary risk factors in 4, and preoperative evaluation in 3. All patients underwent a graded exercise test on a treadmill using a standard Bruce protocol and achieved 85% of the maximal predicted heart rate with no chest pain or electrocardiographic changes suggestive of ischemia. The exercise test showed each patient to have less than a 5% probability

Received May 11, 1999; revision accepted Nov. 1, 1999.

For correspondence or reprints contact: Luis I. Araujo, MD, Hospital of the University of Pennsylvania, Rm. 110, Donner Bldg., 3400 Spruce St., Philadelphia, PA 19104.

of coronary disease (*13*), and no patient underwent cardiac catheterization.

Exercise Testing and Imaging Protocol

Patients fasted for at least 8 h before the exercise test. Imaging was performed with a rest–stress protocol. At least 60 min after the injection of 296–370 MBq ^{99m}Tc-sestamibi, rest images were obtained. Approximately 60–90 min later, patients began the exercise test, and 666–888 MBq ^{99m}Tc-sestamibi were injected at the peak of exercise. Exercise was continued for at least 1 min after the injection. All the images compared were acquired approximately 60 min later.

Image Acquisition and Processing

All SPECT studies were acquired and processed with a triple-head 3000 XP scanner (Picker International, Inc., Cleveland Heights, OH) and an Odyssey VP computer (Picker International) equipped with a simultaneous transmission and emission protocol. This protocol uses all 3 head units for emission detection, and 1 of the heads also detects transmission. A linear external source of energy filled with ^{153}Gd placed at the focal point of one of the 3 high-resolution fanbeam collimators was used to obtain transmission images. Projection images were acquired every 3° for 10 s using an elliptic orbit over 360° (120 projections in 20 min). Energy peaks were set at 140% ± 10% keV for the emission and 90% ± 20% keV for the transmission images. Six raw data files were acquired (2 energy windows in each of the 3 heads) and stored for further processing. Tomographic images were then reconstructed using 4 different protocols. The first, a 180° protocol, used images acquired from a conventional 180° acquisition from the 150° (right anterior oblique) position to the 30° (left posterior oblique) position, the filtered backprojection algorithm for tomographic reconstruction, and a low-pass postreconstruction filter on the transaxial images. The second, a 360° filtered backprojection reconstruction (FBP) protocol, used all 120 projections to reconstruct the tomograms, which were processed with filtered backprojection without AC and with a postreconstruction low-pass filter. The third, a 360° iterative reconstruction (IT) protocol without AC, used all 120 projections and a maximum-likelihood expectation maximization algorithm but no postreconstruction filtering or AC. The fourth, an AC protocol, processed all 120 projections with IT, a maximum-likelihood expectation maximization algorithm, and AC. All images were resliced to obtain the horizontal long-axis, vertical long-axis, and short-axis views.

Image Quantification and Data Analysis

Basal, midventricular, and apical stress short-axis images were selected for quantitative analysis. Eight circular regions of interest, which included at least 2 pixels (pixel size, 5.06 × 5.06 × 5.06 mm), were placed in each short-axis view, and a set of 24 data points (counts per pixels) was obtained for each patient. An average count per pixel was obtained from the 24 regions of interest, and the measured counts were normalized to the average of each patient. Two additional regions of interest were also placed along the vertical long axis to evaluate the anteroapical and inferoapical segments. Each normalized regional value represented the ratio of that region from the average of the entire myocardium. This normalized value was used for all comparisons.

Statistical Analysis

All values were expressed as mean ± SD. ANOVA was used to establish differences among protocols. The Student *t* test was used to assess differences among the same regions processed with different protocols.

RESULTS

Average and SD of the normalized data values for each of the 24 regions analyzed are depicted in a bull's-eye graph in Figure 1 for women and men with the 4 image acquisition and processing protocols.

Comparison Between 180° and 360° FBP Images

The average anterior wall value, from base to apex, appeared to be significantly higher and closer to unity in the 360° FBP images than in the 180° images in both women and men (0.96 ± 0.08 versus 0.87 ± 0.07 for women, $P \leq 0.001$; 1.03 ± 0.06 versus 0.96 ± 0.08 for men, $P \leq 0.01$). The segments with the greatest differences were the distal anterior wall in women (0.99 ± 0.08 versus 0.89 ± 0.06, $P \leq 0.0001$) and the midanterior segment men (1.01 ± 0.05 versus 0.89 ± 0.06, $P \leq 0.0005$).

The septum appeared to be significantly lower and closer to unity in 360° FBP images than in 180° images, again for both women and men (0.97 ± 0.06 versus 1.03 ± 0.09 in women, $P \leq 0.01$; 0.98 ± 0.06 versus 1.05 ± 0.07 in men, $P \leq 0.01$). The septal segment most affected in both men and women was the mid septum. The inferior and lateral segments did not exhibit significant differences with these 2 methods.

Statistically significant differences in uniformity were observed with both methods. In 180° images, the distal anterior wall was lower in women than in men (0.89 ± 0.06 versus 1.03 ± 0.08, $P \leq 0.0001$) and the entire inferior wall was lower in men ($P \leq 0.0001$ for all 3 inferior segments). In 360° FBP images, the distal and midanterior wall segments were lower in women ($P \leq 0.001$) and, again, the entire inferior wall was lower in men ($P \leq 0.001$).

Comparison Between 360° FBP Images and 360° IT Images Without AC

In IT images without AC, the anterior wall appeared to be higher most prominently in the midanterior wall segments in women (1.05 ± 0.07 versus 0.94 ± 0.08, $P \leq 0.0001$) and lower in the basal septum and basal lateral wall ($P \leq 0.001$).

In men, the most prominent change was observed in the inferior wall, where higher values, which were closer to unity, were found in IT images without AC ($P \leq 0.0005$ and 0.001 for the mid and distal inferior segments, respectively). In addition, the lateral wall was lower and closer to unity, with the most prominent change being in the basal and midlateral segments ($P \leq 0.0001$ and 0.01, respectively).

Again, similar differences between men and women were observed with both methods; however, the statistical difference was found to be less marked (e.g., the inferobasal segment was lower, with 360° FBP images at the 0.0001 level and 360° IT images without AC at the 0.05 level).

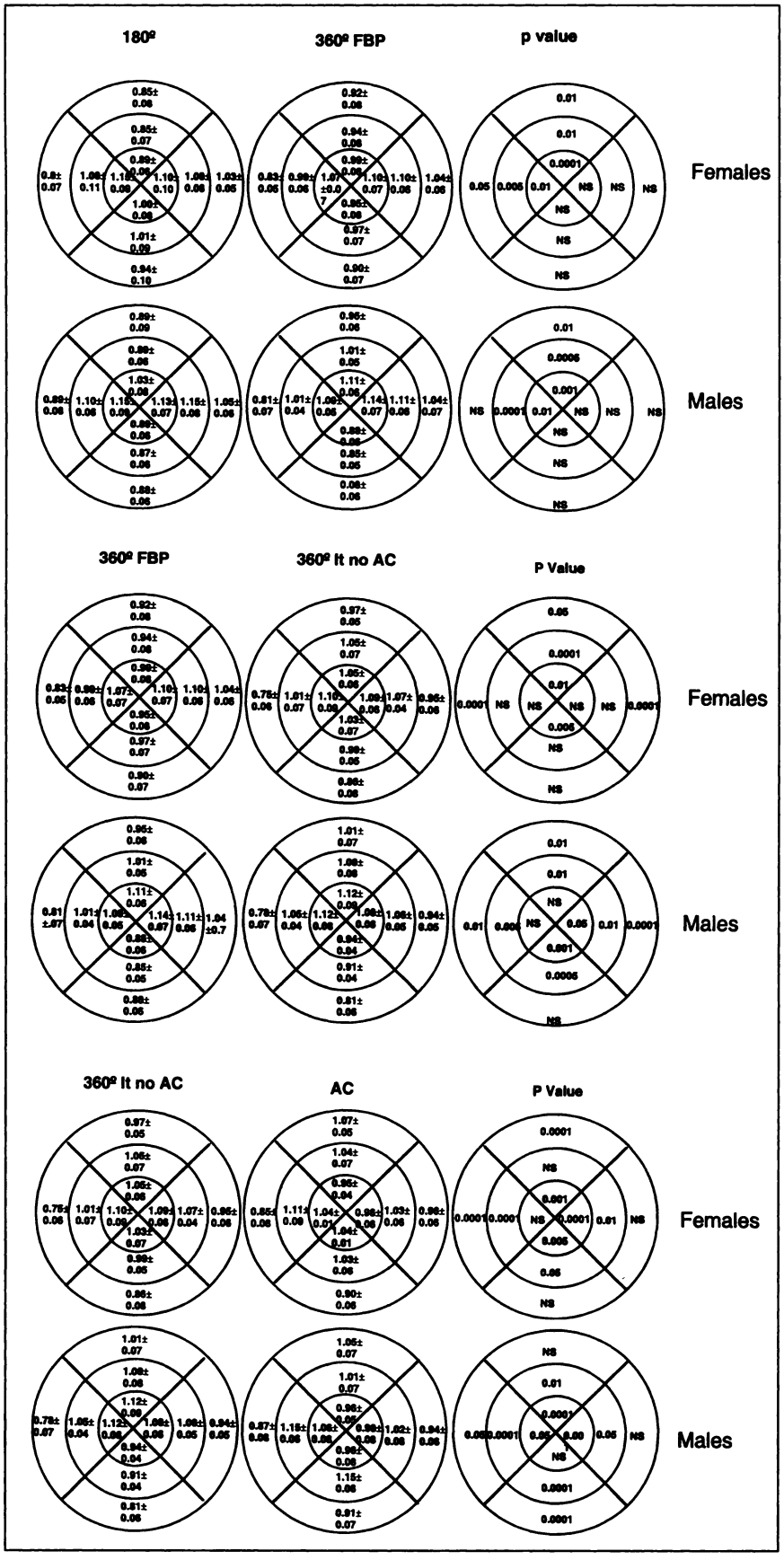

FIGURE 1. Graphic bull's-eye representation of average normalized data obtained for all patients for all 3 short-axis views (base, mid, and apex). Comparisons were made for all 4 image processing methods for men and women. Values of *P* are for comparison between image processing methods. NS = not statistically significant.

Comparison Between 360° IT Images Without AC and AC Images

AC resulted in the most uniform set of images, with a significantly lower coefficient of variation than in 360° IT images without AC (12.5% versus 9.9%, $P \leq 0.0001$). When female and male segmental distribution was compared, differences between men and women were no longer present.

Apical Segments

On 180°, 360°, and IT images, the inferoapical segment was consistently lower than the mean in all subjects ($P = 0.0094$, 0.0021, and 0.0024, respectively). However, the inferoapical segment was not different from the mean on AC images. The anteroapical segment was similar to the mean on all 4 sets of images. The mid and distal segments of the inferior wall were lower in men ($P \leq 0.05$ and 0.018, respectively).

In summary, the anterior wall in women and the inferior wall in men are the segments of the left ventricle that are most affected by different image reconstruction techniques (Figs. 2A and B). Incremental benefit is apparent with the progressive use of 360° acquisition protocols; IT; and, finally, AC, for which the most uniform tracer distribution was quantified (Fig. 3).

DISCUSSION

This study showed that the use of a 360° orbit for data acquisition with IT and AC improves image uniformity and eliminates sex differences.

Imaging artifacts from tissue attenuation have presented, for both visual clinical interpretation and quantification of myocardial perfusion images, a challenge that has resulted in a significant decrease in specificity and sensitivity, especially in the territory of the left circumflex artery (*1*). Several investigators described significant sex differences related to attenuation artifacts and different body configuration in women and men. The classic attenuation artifacts include decreased distal anterior wall tracer concentration in women and decreased inferior wall concentration in men. Our data showed a similar regional distribution when AC was not used. However, the most prominent regional differences (i.e., anterior wall in women and inferior wall in men) were progressively smaller when 360° orbits and IT algorithms were used (Fig. 2 and 3).

The use of 180° acquisition orbits has been the standard acquisition technique in SPECT myocardial perfusion imaging over the last several years. Although promoted for thallium imaging, this technique has remained controversial. Eisner et al. (*14*) suggested that 180° acquisitions would

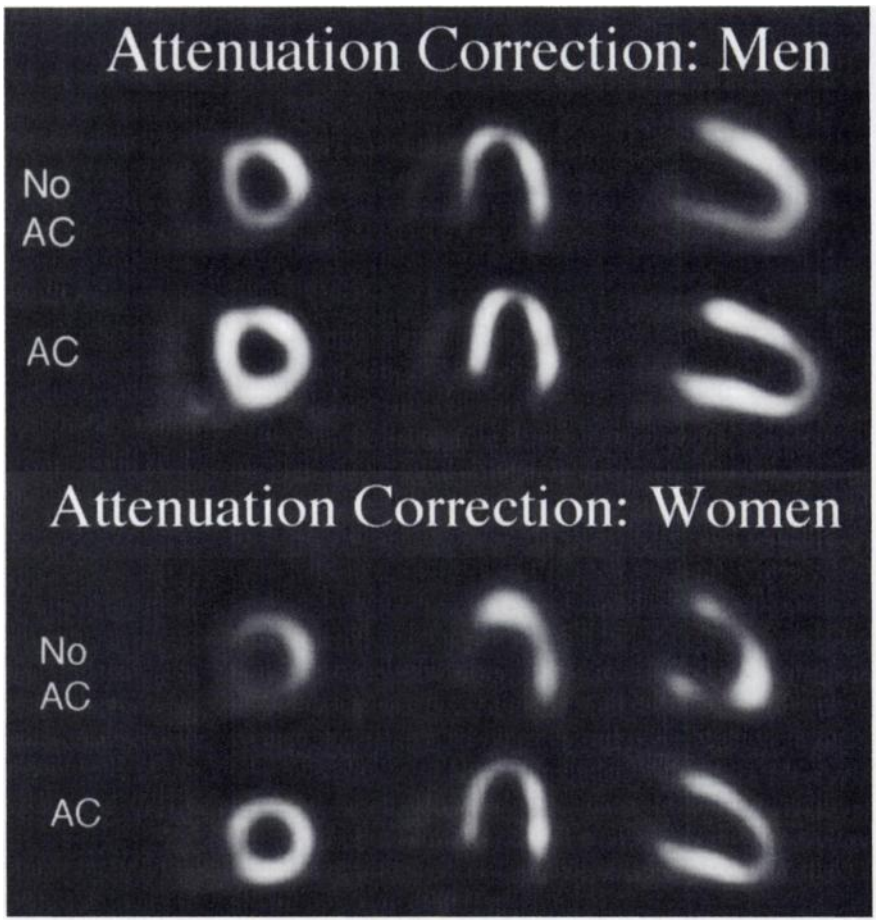

FIGURE 2. Representative midventricular slices along short axis, vertical long axis, and horizontal long axis of men and women from study group. In top row are images with IT and no AC; in bottom row are same slices with IT and AC. AC images show better uniformity.

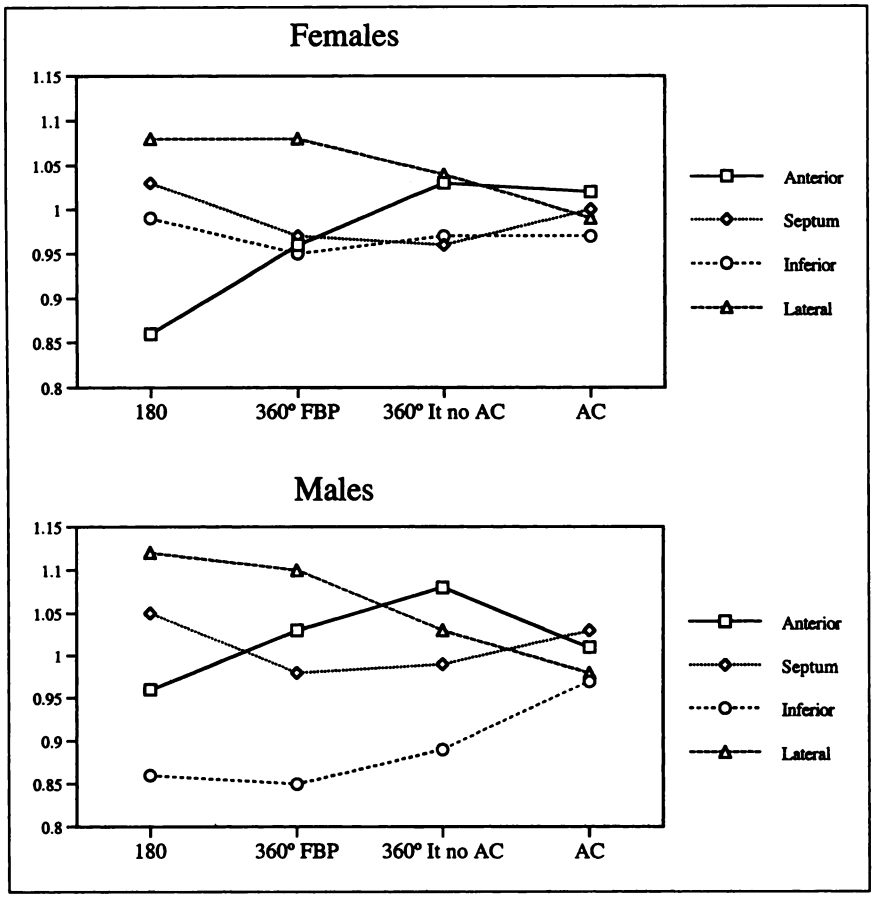

FIGURE 3. Graphs show average values of 4 left ventricular regions in women and men, including base, mid, and apical slices, with 4 methods used for image processing. Greater uniformity is obtained with 360° acquisition, and best results are obtained with AC.

result in a better signal-to-noise ratio (*2*), but Go et al. (*15*) found an increased number of imaging artifacts. Current SPECT scanners are equipped with multiple detectors that allow image acquisition with 180° or 360° orbits in shorter or similar scanning times depending on the chosen protocol. In this study, we showed that 180° acquisition of ^{99m}Tc-sestamibi images resulted in a set of images with the least uniformity and the greatest differences between men and women. Furthermore, 360° acquisition protocols with IT and AC resulted in the most uniform images and no sex differences. This study was performed using a triple-head system equipped with high-resolution fanbeam collimators and a simultaneous transmission and emission protocol for acquisition and image processing provided by the manufacturer and commercially available. Initial development and validation of the AC procedure was performed by Datz et al. (*10*) and showed the effectiveness of the AC protocol in phantom studies. More recently, using similar equipment but slightly different procedures, Ficaro et al. (*12*) showed improved diagnostic accuracy of myocardial perfusion images with AC in a diverse group of patients with a wide range of coronary artery disease. That study also analyzed a group of patients with a low likelihood of coronary artery disease. Our results agree with the observations of Ficaro et al.

This study was an initial observation on the usefulness of the new acquisition protocols with a 360° orbit and simultaneous AC in a few patients with a low likelihood of coronary artery disease. A larger group of patients needs to be thoroughly analyzed, and a new control database with the current techniques needs to be implemented. A direct comparison of 360° images with AC and 180° images with AC, however desirable, was not possible because of equipment limitations.

CONCLUSION

This study showed that the use of 360° acquisition protocols with IT and AC resulted in a more uniform apparent ^{99m}Tc-sestamibi myocardial distribution in a group of patients with a low likelihood of coronary artery disease. The previously described sex differences were no longer observed. The greatest impact of AC was in the inferior and inferolateral regions in men and in the distal anterior wall in women. This method may significantly improve the diagnostic accuracy of myocardial perfusion imaging. Furthermore, a quantitative approach without the necessity of sex-specific databases can be applied for the evaluation of the extent and severity of perfusion defects. Further clinical evaluation with various AC techniques is required.

REFERENCES

1. Van Train KF, Areeda J, Garcia EV, et al. Quantitative same-day rest-stress technetium-99m-sestamibi SPECT: definition and validation of stress normal limits and criteria for abnormality. *J Nucl Med.* 1993;34:1494–1502.

2. Dunn R, Wolf L, Wagner S, Botvinick E. The inconsistent pattern of thallium defects: a clue to a false positive perfusion scintigram. *Am J Cardiol.* 1981;48:224–232.
3. Eisner RL, Tamas MJ, Clononger K, et al. Normal SPECT thallium-201 bulls-eye display: gender differences. *J Nucl Med.* 1988;29:1901–1909.
4. Demer LI, Gould KL, Goldstein RA. Assessment of coronary artery disease severity by positron emission tomography: comparison with quantitative angiography in 193 patients. *Circulation.* 1989;79:825–835.
5. Go RT, Marwick TH, MacIntyre WJ. A prospective comparison of rubidium-82 PET and thallium-201 SPECT myocardial perfusion imaging utilizing a single dipyridamole stress in the diagnosis of coronary artery disease. *J Nucl Med.* 1990;31:1899–1905.
6. Steward RE, Schwaiger M, Molina E. Comparison of rubidium-82 positron emission tomography and thalium-201 SPECT imaging for the detection of coronary artery disease. *Am J Cardiol.* 1991;67:1303–1310.
7. Frey EC, Tsui BM, Perry JR. Simultaneous acquisition of emission and transmission data for improved Tl-201 cardiac SPECT imaging using a Tc-99m transmission source. *J Nucl Med.* 1992;33:2238–2245.
8. Jaszczack RJ, Gilland DR, Hanson MW, Jang S, Greer KL, Coleman RE. Fast transmission CT for determining attenuation maps using collimated line source, rotatable air-copper-lead attenuators and fan-beam collimators. *J Nucl Med.* 1993;34:1577–1586.
9. Tan B, Bailey DL, Meikle SR, Ebelt S, Fulton RR, Hutton BF. A scanning linear source for simultaneous transmission and emission measurements in SPECT. *J Nucl Med.* 1993;34:1752–1760.
10. Datz FL, Gullberg GT, Zeng GL, et al. Application of convergent-beam collimator and simultaneous transmission emission tomography to cardiac single-photon emission computed tomography. *Semin Nucl Med.* 1994;24:17–37.
11. Shepp LA, Vardi Y. Maximum likelihood reconstruction for emission tomography. *IEEE Trans Med Imaging.* 1982;1:113–122.
12. Ficaro EP, Fessler JA, Shreve PD, Kritzman JN, Rose PA, Corbett JR. Simultaneous transmission/emission myocardial perfusion tomography: diagnostic accuracy of attenuation-corrected Tc-99m-sestamibi single-photon emission computed tomography. *Circulation.* 1996;93:463–473.
13. Diamond GA, Forrester JS. Analysis of probabilities as an aid in the clinical diagnosis of coronary artery disease. *N Engl J Med.* 1979;300:1350–1358.
14. Eisner RL, Nowak DJ, Pettigrew R, Fajman W. Fundamentals of 180° acquisition and reconstruction in SPECT imaging. *J Nucl Med.* 1986;27:1717–1728.
15. Go RT, MacIntyre WJ, Houser TS, et al. Clinical evaluation of 360° and 180° data sampling techniques for transaxial thallium-210 myocardial perfusion imaging. *J Nucl Med.* 1985;26:695–706.